

# Production of $\chi_b$ -mesons at LHC

A.K. Likhoded<sup>†1</sup>, A.V. Luchinsky<sup>‡1</sup>, and S.V. Poslavsky<sup>§1</sup>

<sup>1</sup>*Institute for High Energy Physics, Protvino, Russia*

In the present paper we discuss the  $P$ -wave bottomonium production within both color octet and color singlet models in NLO at LHC energies. We calculate the cross section and the transverse momentum distributions for the  $\chi_{1,2b}$  states. We obtain, that the ratios of bottomonium and charmonium spin states production are fundamentally complementary at different  $p_T$  scales. We give predictions for the ratio of the  $n = 2$  and  $n = 1$  radial excitations production cross sections.

PACS numbers.: 14.40.Pq, 14.40.Nd, 13.85.-t

## 1 Introduction

Studies of heavy quarkonia give a deeper understanding of the Quantum Chromodynamics. In the recent measurements made by ATLAS [1] and D0 [2] Collaborations the new data for the  $b\bar{b}$  systems was obtained. The radial excitation of the  $P$ -wave  $\chi_b$  states was observed in radiative transitions to the  $S$ -wave  $\Upsilon$  states, while  $\chi_b(3P)$  was seen for the first time. The  $\chi_b$  system is a triplet of closely spaced states with total spin  $J = 0, 1$  and  $2$ , that were not observed separately at ATLAS yet. Usually, only  $1^{++}$  and  $2^{++}$  can be detected, since  $0^{++}$  state has very small radiative branching fraction. So, in the present paper, we shall focus on a production of  $1^{++}$  and  $2^{++}$  charmonium and bottomonium states. We shall consider the production with high transverse momentum of the final quarkonium.

Main contribution to the production processes at high energies ( $\sim$  TeV) is given by gluon-gluon subprocesses. The problem of the quarkonia production can be divided into two parts. The first part of the problem is to obtain the nonzero transverse momentum of the final quarkonia using the integrated partonic distributions (PDFs). The second part consists in the hadronization process, i.e. formation of the quarkonia with certain quantum numbers. For example, let us consider the production of the  $|^3S_1\rangle$  ( $1^{--}$ ) state. The colorless state with such quantum numbers cannot be produced from two gluons because of the charge parity conservation. So, the production of the color singlet state with the additional emission of a gluon in

---

<sup>†</sup>Anatolii.Likhoded@ihep.ru

<sup>‡</sup>Alexey.Luchinsky@ihep.ru

<sup>§</sup>stvlpos@mail.ru

the final state was introduced [3, 4] to explain the quarkonia production. Additional emission of the gluon gives the  $p_T$ -distribution and removes the prohibition of the  $1^{--}$  state production. It is well known, that such a model, in its naive understanding, is in the contradiction with the experimental data at high  $p_T$ . In the case of  $P$ -wave meson production the situation is different:  $0^{++}$  and  $2^{++}$  states can be produced from two gluons, but in the collinear approximation (with integrated over  $p_T$  partonic distributions) the transverse momentum distribution of final quarkonium cannot be obtained. Moreover,  $|^3P_1\rangle$  state cannot be produced due to Landau-Yang theorem, which forbids the production of axial meson from two massless gluons. These problems have led to the approach, known as  $k_T$ -factorization [5, 6, 7, 8], in which unintegrated partonic distributions are used. However, we think that such an approach should play a significant role at the low  $p_T$  region only, while in the high  $p_T$  region the dominant contribution to the  $p_T$  is given by the processes with emission of a single hard gluon in the final state.

In this paper we try to resolve the above problems considering a set of diagrams, in which high  $p_T$  is achieved by the emission of single hard gluon, mostly from the initial state. It turns out that all three  $P$ -waves states, including  $1^{++}$  are allowed. As we shall see, the color-singlet contributions give  $p_T$  dependence, which is similar to the experiment data for  $\chi_c$  mesons, for example from CDF [9], but the absolute normalization of the cross section is several times smaller than in the experiment. To resolve this contradiction we took into account the color-octet contributions to the cross sections. In the next section we show that if we consider the color-octet matrix elements as free parameters, the good agreement with the experimental data can be obtained for the case of  $\chi_c$ , and the predictions for the  $\chi_b$  states can be provided. Next, we consider the cross section ratio of the  $2^{++}$  and  $1^{++}$  production both for  $\chi_c$  and  $\chi_b$ , which was recently measured for charmed mesons at the LHCb detector [10], and show, that our approach gives the value, lying at the lower limit of uncertainties of the LHCb data. There is no such experimental data on the bottomonium production yet and our result should be considered as the theoretical predictions for further experiments. Next, we consider the ratio of the  $n = 2$  and  $n = 1$  radial excitations, which is not measured yet and present our theoretical predictions.

## 2 $\chi_c$ production at high $p_T$

The cross section of heavy quarkonium production in hadronic interaction can be expressed through the cross sections of hard subprocesses:

$$d\sigma [pp \rightarrow \mathcal{Q} + X] = \int dx_1 dx_2 f_g(x_1; Q) f_g(x_2; Q) d\hat{\sigma}[\mathcal{Q}] \quad (1)$$

Here,  $\mathcal{Q}$  is one of the  $|^3P_J\rangle$  states,  $x_{1,2}$  are the momentum fractions of the partons,  $f_g(x_{1,2}; Q)$  are the gluon distribution functions in initial hadrons, and  $d\hat{\sigma}[\mathcal{Q}]$  is the cross section of the meson production at the partonic level.

As already mentioned in the Introduction, in order to obtain nonzero transverse momentum of final quarkonia using the usual partonic distributions, it is necessary to consider next to leading order subprocesses with the emission of an additional gluon, i.e.  $gg \rightarrow \chi_{bJ}g$ . The corresponding Feynman diagrams are shown in Fig. 1. The partonic cross sections of these

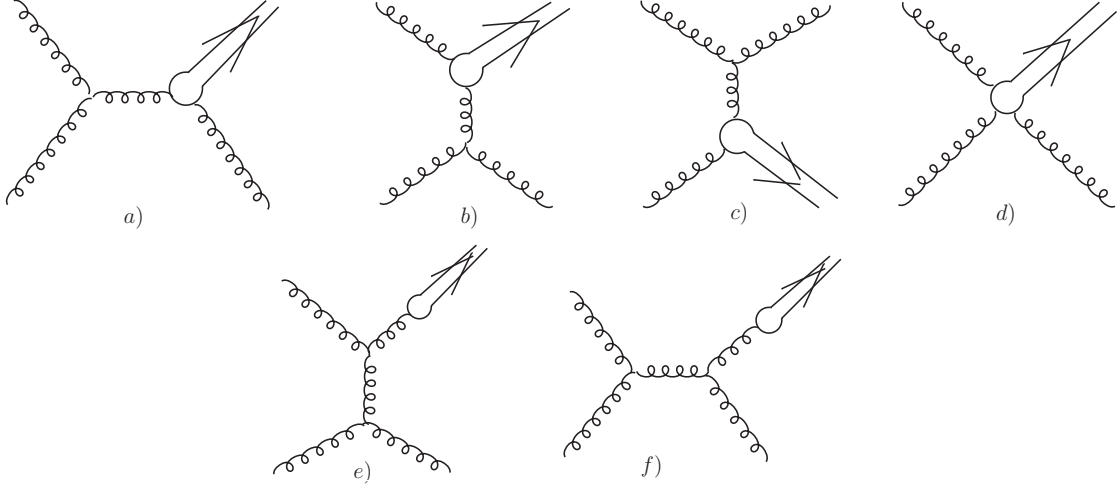


**Figure 1:** The Feynman diagrams of the  $gg \rightarrow \chi_b g$  subprocesses. The first four diagrams are valid both for color-singlet and color-octet mechanism, while the last two diagrams corresponds to the octet production only.

reactions were calculated by a number of authors [11, 12, 13, 14], but result presented in [13] disagrees with others works. The reason is that diagrams shown in Fig.1 include 3-gluon vertex and the additional ghost contributions should be included. Our calculations performed in QCD axial gauge (which does not require additional ghosts contributions) reproduces [11, 12, 14] results.

It should be noted, that the above expressions depend on two scale parameters: the renormalization scale  $\mu$  in strong coupling constant  $\alpha_S(\mu)$  and the maximum transverse momentum of collinear gluons  $Q$  in structure functions  $f(x, Q)$ . At low energies the variation of these scale parameters leads to significant variation of the total cross sections [15], while for the energies about several TeVs the dependence is not crucial. In our work we will use the value  $Q = \mu = M$ , where  $M$  is the mass of the heavy quarkonium. Also we shall neglect the mass difference between states from same  $\chi_J(nP)$  triplet.

It is known, that color-singlet model of  $q\bar{q}$  pair hadronization into observable meson does not fully describe experimental data. The reason is that color-singlet is only the first approximation in the Fock structure of quarkonium state [16]:

$$\begin{aligned}
|^{2S+1}L_J\rangle &= O(1)|^{2S+1}L_J^{[1]}\rangle \\
&+ O(v)|^{2S+1}(L \pm 1)_{J'}^{[8]}g\rangle \quad (\text{E1}) \\
&+ O(v^2)|^{2(S \pm 1)+1}L_{J'}^{[8]}g\rangle \quad (\text{M1}) \\
&+ O(v^2)|^{2S+1}L_J^{[1,8]}gg\rangle \quad (\text{E1} \times \text{E1}) \\
&+ \dots \quad (2)
\end{aligned}$$

where  $v$  is the relative velocity of quarks in heavy quarkonium. In the above expression E1 and M1 are electric ( $\Delta L = 1, \Delta S = 0$ ) and magnetic ( $\Delta S = 1, \Delta L = 0$ ) transitions respectively.

In the case of  $\chi_c$  mesons equation (2) gives:

$$\begin{aligned}
|\chi_{cJ}\rangle &= \langle \mathcal{O}^{\chi_{cJ}}[{}^3P_J^{[1]}] \rangle |{}^3P_J^{[1]}\rangle + \langle \mathcal{O}^{\chi_{cJ}}[{}^3S_1^{[8]}] \rangle |{}^3S_1^{[8]}\rangle + \\
&+ \langle \mathcal{O}^{\chi_{cJ}}[{}^1P_1^{[8]}] \rangle |{}^1P_1^{[8]}\rangle + \sum_{J'} \langle \mathcal{O}^{\chi_{cJ}}[{}^3P_{J'}^{[8]}] \rangle |{}^3P_{J'}^{[8]}\rangle + \dots
\end{aligned} \tag{3}$$

Here the first two terms are order of  $O(v)$ , and next two terms are of order  $O(v^2)$ .

In Fig. 2 the contributions from different states in (3) to the  $p_T$ -distributions of  $J/\psi$  mesons produced via  $\chi_c$  radiative decays:

$$\frac{d\sigma}{dp_T}[p\bar{p} \rightarrow \chi_c + X \rightarrow J/\psi + X] = \text{Br}[\chi_{c1}] \frac{d\sigma}{dp_T}[p\bar{p} \rightarrow \chi_{c1} + X] + \text{Br}[\chi_{c2}] \frac{d\sigma}{dp_T}[p\bar{p} \rightarrow \chi_{c2} + X].$$

are shown in comparison with the CDF experimental data [9]. The octet  $|{}^3S_1^{[8]}\rangle$  state gives  $p_T$ -distribution approximately described by  $\sim 1/p_T^4$ , which is far different from the experimental one, which, in turn, is approximately described by  $\sim 1/p_T^6$ . So, in order to fit the experimental data, we should assume, that  $|{}^3S_1^{[8]}\rangle$  gives a negligibly small contribution in the considered  $p_T$  interval and plays role for higher  $p_T$  only. The other states from the Fock expansion (3), including color-singlet, have the  $p_T$ -distribution similar to the experimental measurement. In order to fit the experimental data, we used CDF data for the  $\chi_c$  production and the available data for the cross section ratio of  $\sigma(\chi_{c2})/\sigma(\chi_{c1})$  [10, 24, 25] (see next section and Fig. 4). The singlet contribution is determined by the singlet matrix element  $\mathcal{O}[{}^3P_J^{[1]}]$ , which is connected with the derivative of the radial part of the wave function at the origin:

$$\langle \mathcal{O}^{\chi_{cJ}}[{}^3P_J^{[1]}] \rangle = \frac{3}{4\pi} (2J+1) |R'(0)|^2.$$

For the last one we took the value derived from the  $\chi_{c2}$  photonic width in LO:

$$|R'(0)|^2 = 0.075 \text{ GeV}^5.$$

The octet matrix elements for  $|{}^3S_1^{[8]}\rangle$  satisfies the multiplicity relations

$$\langle \mathcal{O}^{\chi_{cJ}}[{}^3S_1^{[8]}] \rangle = (2J+1) \langle \mathcal{O}^{\chi_{c0}}[{}^3S_1^{[8]}] \rangle$$

For the last one we obtained from our fit the following value:

$$\langle \mathcal{O}^{\chi_{c0}}[{}^3S_1^{[8]}] \rangle \lesssim 2 \times 10^{-5} \text{ GeV}^3 \tag{4}$$

Since  $|{}^1P_1^{[8]}\rangle$  and  $|{}^3P_J^{[8]}\rangle$  states have similar  $p_T$ -dependence, they could not be resolved separately and only a linear combination of the corresponding octet matrix elements can be determined. In the notations of [14] we obtain the following values for the non-perturbative parametres:

$$\langle R^{\chi_{c0}}[{}^1P_1^{[8]}] \rangle = \langle R^{\chi_{c0}}[{}^3P_{J'}^{[8]}] \rangle = 0.01 \text{ GeV}^5 \tag{5}$$

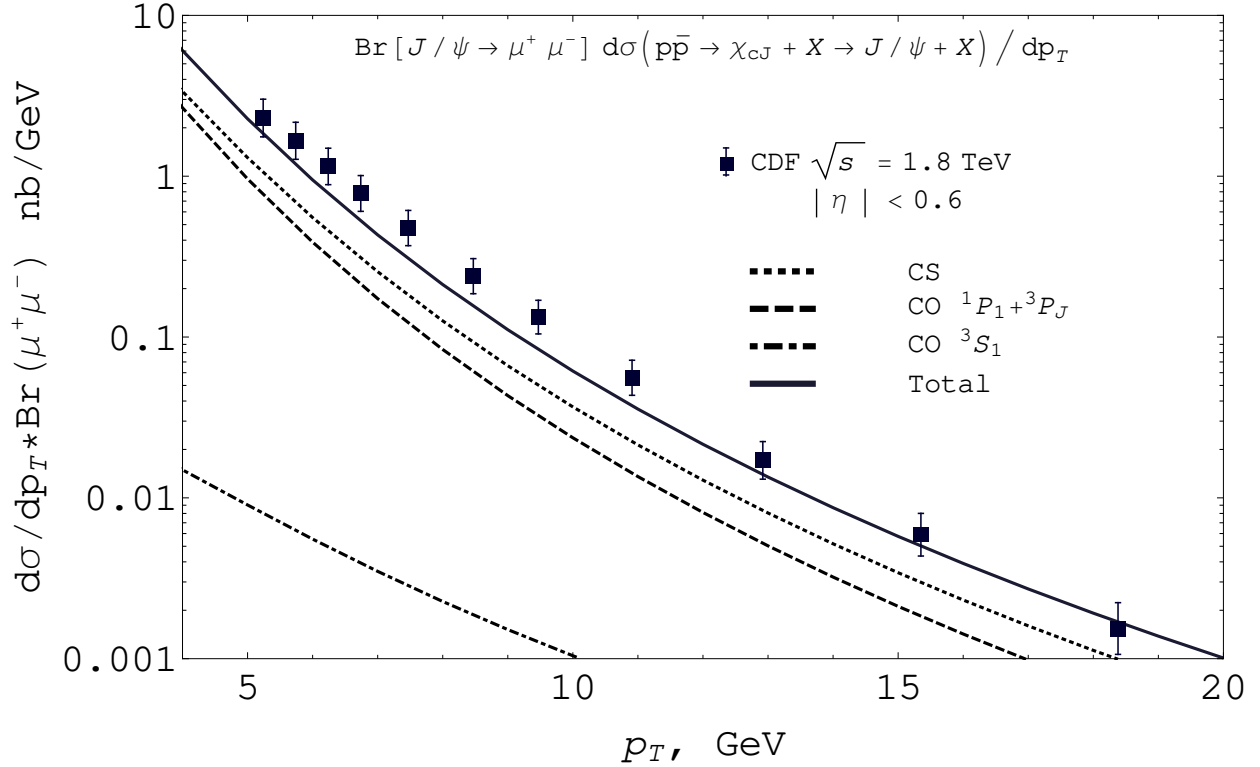


**Figure 2:** Contributions to the  $\chi_c$  production from different states. Dotted line is color singlet contribution. Dashed line is a contribution from the octet  $|^3P_J^{[8]}\rangle$  and  $|^1P_1^{[8]}\rangle$  states. Dot-dashed line is color-octet  $|^3S_1^{[8]}\rangle$  state contribution. Solid line is a sum over all contributions. Experimental points are taken from CDF report [9].

The last result is independent on  $J'$ . Taking into account statistical weight of the  $\chi_{cJ}$ -state the corresponding parameters for the  $\chi_{cJ}$  production can be recovered:

$$\begin{aligned} \langle R^{\chi_{cJ}}[{}^1P_1^{(8)}] \rangle &= (2J+1) \langle R^{\chi_{c0}}[{}^1P_1^{(8)}] \rangle \\ \langle R^{\chi_{cJ}}[{}^3P_{J'}^{(8)}] \rangle &= (2J+1) \langle R^{\chi_{c0}}[{}^3P_{J'}^{(8)}] \rangle \end{aligned}$$

At this point we need to discuss the results of our fit. In most works (see, for example, review [17]) it is accepted to neglect the  $P$ -wave octet contributions due to the velocity power counting rules, and the following ranges of values of non-perturbative matrix element for the  $|^3S_1^{[8]}\rangle$  state are considered:

$$\langle \mathcal{O}^{\chi_{c0}}[{}^3S_1^{[8]}] \rangle \sim (0.1 - 0.5) \times 10^{-2} \text{ GeV}^3$$

Nevertheless, we state that  $|^3S_1^{[8]}\rangle$  contribution gives inappropriate  $p_T$ -dependence to describe the experimental data and therefore octet  $P$ -wave contributions should be included.

On the other hand, the non-perturbative value of the octet  $|^3S_1^{[8]}\rangle$  contribution from work [8] is closer to our result:

$$\langle \mathcal{O}^{\chi_{c0}}[{}^3S_1^{[8]}] \rangle \sim 2 \times 10^{-4} \text{ GeV}^3,$$

but the derivative of the radial part of the wave function at the origin is about several times bigger than ours:

$$|R'(0)|^2 \sim 0.37 \text{ GeV}^5,$$

so the almost entire contribution is given by the singlet term. We think, that this value is unreasonably high and does not agree with experimental data. Possible reason of the contradiction is that authors derive this value from the photonic width including QCD radiative correction. It is clear, that using such approach the radiative corrections to the initial state production should be considered on a par with radiative corrections in the final state, but this was not performed.

### 3 $\chi_b$ production at high $p_T$

Let us proceed to the  $\chi_b$  mesons production. The picture of the bottomonium production is almost the same as in the charmonium case. The only difference is that probabilities in Fock expansion (3) have different values. We shall assume, that relative contributions from different Fock states are similar to charmonium mesons and do not depend on the radial excitation number  $n$ . So, for example,

$$\frac{\langle \mathcal{O}[{}^3P_J^{[8]} \rightarrow \chi_c] \rangle}{\langle \mathcal{O}[{}^3P_J^{[1]} \rightarrow \chi_c] \rangle} = \frac{\langle \mathcal{O}[{}^3P_J^{[8]} \rightarrow \chi_b(nP)] \rangle}{\langle \mathcal{O}[{}^3P_J^{[1]} \rightarrow \chi_b(nP)] \rangle} \quad (6)$$

From the dimension analysis, it is clear, that

$$\frac{\langle \mathcal{O}[{}^3S_1^{[8]}] \rangle}{\langle \mathcal{O}[{}^3P_J^{[1]}] \rangle} \sim \frac{1}{M^2}$$

So, for  $|{}^3S_1\rangle$  we take

$$\frac{\langle \mathcal{O}[{}^3S_1^{[8]} \rightarrow \chi_c] \rangle}{\langle \mathcal{O}[{}^3P_J^{[1]} \rightarrow \chi_c] \rangle} = \frac{M_{\chi_b}^2}{M_{\chi_c}^2} \frac{\langle \mathcal{O}[{}^3S_1^{[8]} \rightarrow \chi_b(nP)] \rangle}{\langle \mathcal{O}[{}^3P_J^{[1]} \rightarrow \chi_b(nP)] \rangle} \quad (7)$$

In Fig. 3 we show our results for the transverse momentum distributions for axial and tensor bottomonium. For the derivative of the wave function at the origin we take

$$|R'_n(0)|^2 = 1 \text{ GeV}^5,$$

which is in agreement with potential models, presented in Tab. 1. For other non-perturbative parameters we use values obtained in the previous section and evaluated with (6) and (7). Presented curves allow one to easily reconstruct the distributions for any  $|R'_n(0)|$  value, by simply multiplying on the corresponding factor from Tab. 1.

In Fig. 4 the  $p_T$ -dependence of the  $\chi_Q(J=2)/\chi_Q(J=1)$  ratio is depicted. In case of charmonium mesons we compare our results with the LHCb data [10], CDF data [24] and CMS preliminary [25]. Both for  $(c\bar{c})$  and  $(b\bar{b})$  mesons we present the cross section ratio in the rapidity

	[18]	[19]	[20]	[21]	[22]	[23]
$\chi_b(1P)$	0.71	1.02	2.03	0.94	0.84	0.51
$\chi_b(2P)$	0.99	0.88	2.2	1.13	0.98	0.25
$\chi_b(3P)$	—	—	2.43	1.17	1.03	—

**Table 1:**  $|R'_{nP}(0)|^2$  (in  $\text{GeV}^5$ ) from different potential models

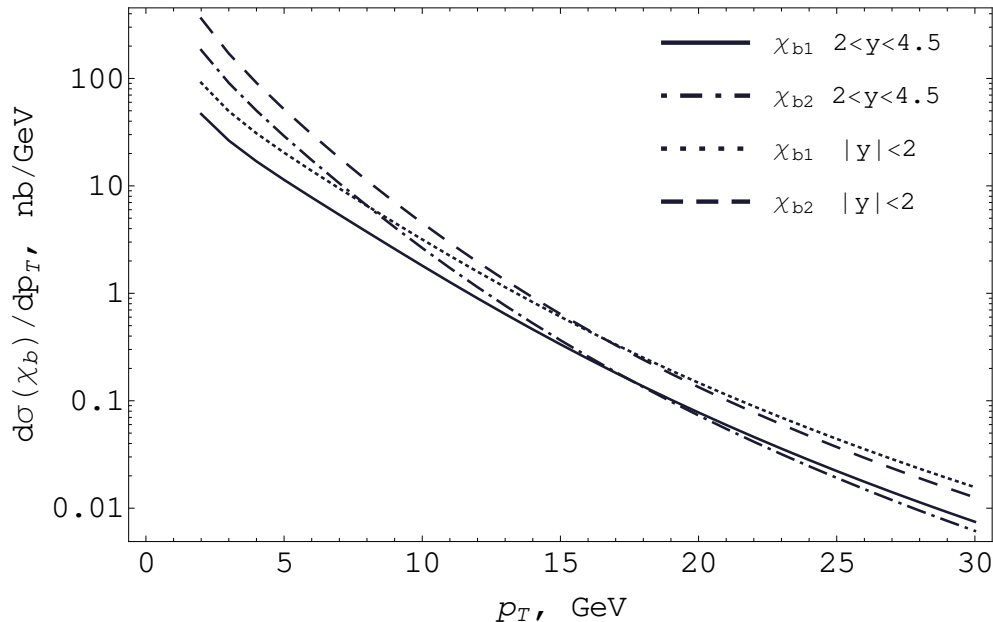


**Figure 3:** Transverse momentum distributions of the  $\chi_{b1}$  and  $\chi_{b2}$  mesons at  $\sqrt{s} = 8$  TeV. The derivative of the wave function at the origin is  $|R'_n(0)|^2 = 1 \text{ GeV}^5$ , which is in agreement with potential models, presented in Tab. 1. Other non-perturbative parameters were obtained in the previous section in the case of charmonium and corresponds to the total curve in Fig. 2 and then evaluated for bottomonium using (6) and (7).

range  $2 < y < 4.5$ , but it is clear that this ratio depends weakly on the rapidity cut, so these predictions should be also valid for another rapidity regions. One can easily see, that within the experimental errors our results for charmonia agree well with experiment, so approach used in our paper is valid. It is clear, that since the cross section is proportional to the  $|R'(0)|^2$  and if the mass gap between  $\chi_J(nP)$  states with different radial numbers  $n$  is neglected, the ratio  $d\sigma[\chi_2(nP)]/d\sigma[\chi_1(nP)]$  does not depend on  $n$  and curves for charmonia and bottomonia presented on Fig. 4 are universal.

One interesting property can be seen from Fig. 4: the bottomonium curve matches the charmonium curve if we perform the rescaling of the  $p_T$  variable:  $p_T \rightarrow (M_{\chi_c}/M_{\chi_b})p_T \approx (1/3)p_T$ . Moreover, this fact is exact model-independent theoretical result, which can be obtained from the dimension analysis. Indeed, the cross section of the quarkonia production depends on three dimensional parameters: hadronic energy, transverse momentum of final quarkonium and its

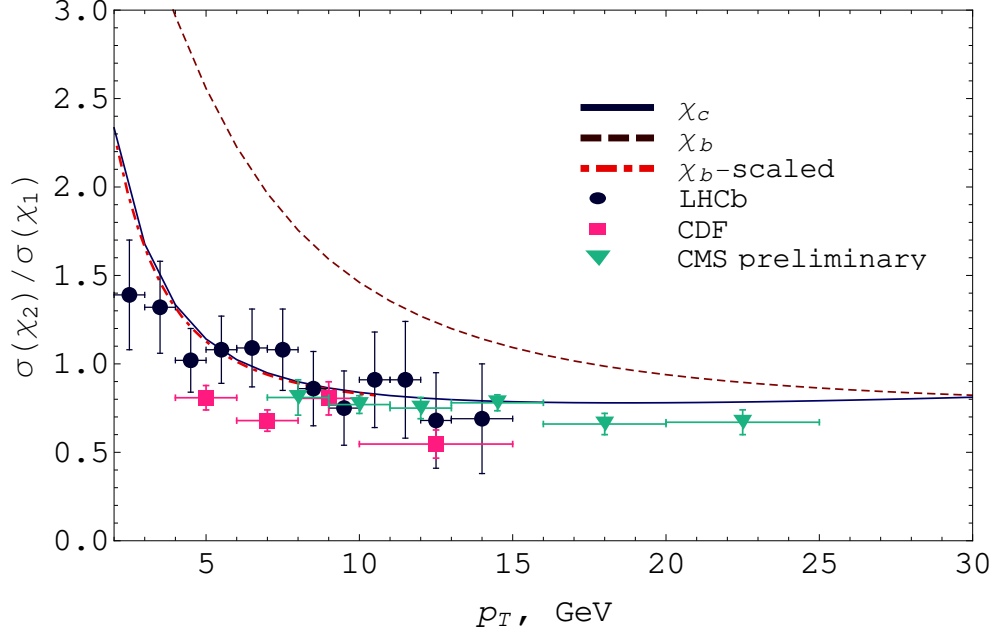


**Figure 4:** Transverse momentum distributions of the  $d\sigma[\chi_2]/d\sigma[\chi_1]$  ratio. Solid and dashed lines stand for charmonium and bottomonium mesons. The dot-dashed line corresponds to the rescaled bottomonium ratio:  $\sigma_{b2}/\sigma_{b1}(M_{\chi_c}/M_{\chi_b} p_T)$ . As it is seen, it almost matches the charmonium curve. The experimental results for charmonium from LHC [10] are shown with dots, CDF [24] — with rectangles, and CMS [25] — with triangles.

mass:

$$\frac{d\sigma_J}{dp_T} \equiv \frac{d\sigma_J}{dp_T}(s, p_T, M)$$

The cross section ratio  $J = 2$  and  $J = 1$  is dimensionless function of these parameters. Hence, we can write:

$$\frac{d\sigma_2(z^2 s, zp_T, zM)}{dp_T} \bigg/ \frac{d\sigma_1(z^2 s, zp_T, zM)}{dp_T} = \frac{d\sigma_2(s, p_T, M)}{dp_T} \bigg/ \frac{d\sigma_1(s, p_T, M)}{dp_T} \quad (8)$$

Taking  $M = M_{\chi_c}$  and  $z = M_{\chi_b}/M_{\chi_c}$ , we obtain

$$\frac{d\sigma_{b2}(zp_T; s)}{dp_T} \bigg/ \frac{d\sigma_{b1}(zp_T; s)}{dp_T} = \frac{d\sigma_{c2}(p_T; s/z^2)}{dp_T} \bigg/ \frac{d\sigma_{c1}(p_T; s/z^2)}{dp_T}. \quad (9)$$

Hence, if we know the charmonium ratio transverse momentum distribution at some c.m. energy  $s$ , we can easily reconstruct the bottomonium ratio distribution at energy  $s (M_{\Upsilon}/M_{J/\psi})^2$ . This relation is not violated by the scale dependence of  $\alpha_s$  and PDFs, since they are canceled in the ratio.

It is intuitively clear, that at least for high energies the ratio weakly depends on  $s$ , since both axial and tensor meson acquire universal behaviour in  $s$ , so the  $s$ -dependence cancels in

this ratio. This argument does not work for low  $s$ , when another partonic channels becomes significant. The value of  $z$  is about  $z \sim 3$ , so the bottomonium distribution at  $\sqrt{s} = 8$  TeV corresponds to the charmonium distribution at  $\sqrt{s} \sim 2.6$  TeV, which is still very high, so the gluonic subprocess dominates. We can expect, that (9) can be approximately rewritten for high energies:

$$\frac{d\sigma_{b2}(zp_T; s)}{dp_T} \bigg/ \frac{d\sigma_{b1}(zp_T; s)}{dp_T} = \frac{d\sigma_{c2}(p_T; s)}{dp_T} \bigg/ \frac{d\sigma_{c1}(p_T; s)}{dp_T}. \quad (10)$$

### 3.1 Radial excitations

Let us now discuss the production of excited  $\chi_b$ -mesons at LHC. Recently  $\chi_b(1P)$ -,  $\chi_b(2P)$ - and  $\chi_b(3P)$ -mesons were observed in  $\Upsilon(1S)\gamma$  and  $\Upsilon(2S)\gamma$  modes by ATLAS Collaboration [1] and D0 [2] Collaboration. In these experiments the radial excitation of the P-wave  $\chi_b$  states was observed in the radiative transitions to the S-wave  $\Upsilon$  states. Unfortunately the exact values of the cross sections were not measured yet, but we can reconstruct them theoretically.

The experimentally observable quantities are:

$$\sigma^{\text{th}} [nP, mS] = \sigma^{\text{th}} [pp \rightarrow \chi_b(nP) + X \rightarrow \Upsilon(mS)\gamma + X] = \sum_{J=0}^2 \text{Br}_J [nP, mS] \sigma_J^{\text{th}} [nP] \quad (11)$$

where the following notations were used:

$$\begin{aligned} \sigma_J^{\text{th}} [nP] &= \sigma^{\text{th}} [pp \rightarrow \chi_{bJ}(nP) + X], \\ \text{Br}_J [nP, mS] &= \text{Br} [\chi_{bJ}(nP) \rightarrow \Upsilon(1S)\gamma]. \end{aligned}$$

The branching fractions of radiative  $\chi_b(1P)$ - and  $\chi_b(2P)$ -mesons decays are known experimentally [26]:

$$\begin{aligned} \text{Br}_1 [1P, 1S] &= 35\% \pm 8\%, & \text{Br}_2 [1P, 1S] &= 22\% \pm 4\%, \\ \text{Br}_1 [2P, 1S] &= 8.5\% \pm 1.3\%, & \text{Br}_2 [2P, 1S] &= 7.1\% \pm 1\%, \\ \text{Br}_1 [2P, 2S] &= 21\% \pm 4\%, & \text{Br}_2 [2P, 2S] &= 16\% \pm 2.4\%. \end{aligned}$$

In the case of scalar bottomonium the branching fractions are small, so we do not include it in the sum (11).

In order to calculate the total cross sections, we should integrate the cross sections distributions obtained in the previous section and presented on Fig. 3 over appropriate  $p_T$  region:  $\Delta < p_T < (s - M^2)/2\sqrt{s}$ . We use experimental values  $\Delta = 12$  GeV for ATLAS ( $|y| < 2$ ) [1], and  $\Delta = 6$  GeV for LHCb ( $2 < y < 4.5$ ) [27]. Using these values we obtained the following prediction for the cross sections:

$$\begin{aligned} (\text{LHCb}) \quad & \frac{1}{|R'_n(0)|^2} \sigma^{\text{th}} [\chi_{b1}(nP)] = 34.4 \frac{\text{nb}}{\text{GeV}^5} & \frac{1}{|R'_n(0)|^2} \sigma^{\text{th}} [\chi_{b2}(nP)] &= 43 \frac{\text{nb}}{\text{GeV}^5} \\ (\text{ATLAS}) \quad & \frac{1}{|R'_n(0)|^2} \sigma^{\text{th}} [\chi_{b1}(nP)] = 5.2 \frac{\text{nb}}{\text{GeV}^5} & \frac{1}{|R'_n(0)|^2} \sigma^{\text{th}} [\chi_{b2}(nP)] &= 5.6 \frac{\text{nb}}{\text{GeV}^5} \end{aligned}$$

and for the ratio  $\sigma[\chi_b(2P)]/\sigma[\chi_b(1P)]$  in both cases:

$$\frac{\sigma^{\text{th}} [2P, 1S]}{\sigma^{\text{th}} [1P, 1S]} = (0.29 \pm 0.01^{\text{th}} \pm 0.1^{\text{br}}) \left| \frac{R'_{2P}}{R'_{1P}} \right|^2,$$

Here the first error is the error of our theoretical method, while the second is the uncertainty in the experimental values of branchings fractions. This ratio is determined by the ratio of  $2P$ - and  $1P$ -states wave function derivatives at the origin (see Table 1). In Table 2 we show the predictions of different potential models for this ratio.

Potential model	Ratio $\chi_b(2P)/\chi_b(1P)$			
[18]	0.4	$\pm$	$0.01^{\text{th}}$	$\pm 0.14^{\text{br}}$
[19]	0.25	$\pm$	$0.01^{\text{th}}$	$\pm 0.1^{\text{br}}$
[20]	0.32	$\pm$	$0.02^{\text{th}}$	$\pm 0.1^{\text{br}}$
[21]	0.34	$\pm$	$0.01^{\text{th}}$	$\pm 0.12^{\text{br}}$
[22]	0.34	$\pm$	$0.01^{\text{th}}$	$\pm 0.12^{\text{br}}$
[23]	0.14			$\pm 0.05^{\text{br}}$

**Table 2:** Theoretical predictions for the ratio of  $\chi_b(2P)$  and  $\chi_b(1P)$  production cross sections in different potential models

In the case of  $\chi_b(3P)$ -mesons production the corresponding branching fractions to  $\Upsilon(1S)$  are not known yet, so we cannot perform similar analysis. However, we can estimate the radiative branching fraction of tensor meson using the following assumptions. We assume, that the main hadronic decay channel of tensor meson is 2-gluon decay:

$$\Gamma[\chi_{b2}(3P) \rightarrow gg] = \frac{128}{5} \alpha_s^2 \frac{|R'_3(0)|^2}{M^4}$$

and the radiative branching fraction of the  $\chi_{b2}(3P)$  is equal to

$$\text{Br}_2 [3P, 1S] = \frac{\Gamma[\chi_{b2}(3P) \rightarrow \Upsilon(1S)\gamma]}{\Gamma[\chi_{b2}(3P) \rightarrow \Upsilon(1, 2, 3S)\gamma] + \Gamma[\chi_{b2}(3P) \rightarrow gg]}$$

The radiative width can be obtained from the potential models [20, 22]. Using the cross section of  $\Upsilon(1S)$  produced via  $\chi_{b1,2}(3P)$  radiative decays

$$\sigma^{\text{th}} [3P, 1S] = \text{Br}_1 [3P, 1S] \sigma_1^{\text{th}} [3P] + \text{Br}_2 [3P, 1S] \sigma_2^{\text{th}} [3P],$$

we can express the unknown branching fraction of the  $\chi_{b1}(3P) \rightarrow \Upsilon(1S)\gamma$  decay through the ratio of the  $3P$  and  $1P$  production cross sections. The results are presented in Table 3, where we denoted

$$\gamma = \frac{\sigma^{\text{th}} [3P, 1S]}{\sigma^{\text{th}} [1P, 1S]}$$

So, if the experimental value of  $\gamma$  is found, the estimation on the radiative width  $\chi_{b1}(3P) \rightarrow \Upsilon(1S)\gamma$  will be found too. Similar estimations can be also performed for the  $\chi_b \rightarrow \Upsilon(2S)\gamma$  processes.

Potential model	Br <sub>2</sub> [3 <i>P</i> , 1 <i>S</i> ]	Br <sub>1</sub> [3 <i>P</i> , 1 <i>S</i> ]
[20]	1.7%	((41 ± 9) γ - 1.3)%
[22]	5.4%	((42 ± 9) γ - 4.1)%

**Table 3:** Branching fractions of  $\chi_b(3P) \rightarrow \Upsilon(1S)\gamma$  decays

## 4 Conclusions

The present paper is devoted to the  $\chi_b$ -meson production in hadronic experiments. Recently ATLAS [1] and D0 [2] Collaborations reported about observation of  $\chi_b(1, 2, 3P)$  states, so theoretical description of these processes is desirable.

In our paper we use both color singlet and color octet models for description of the  $P$ -wave heavy quarkonia production. For high energy reactions these mesons are produced mainly in gluon-gluon interactions and the cross sections of the corresponding processes can be written as a convolution of partonic cross sections and gluon distribution functions in initial hadrons. If one uses usual distribution functions integrated over the gluon transverse momentum and works at leading order (i.e. only  $gg \rightarrow \chi_b$  partonic reactions are considered), the information about the transverse momentum distribution of final quarkonia  $p_T$  is lost. It is clear, that in order to describe this distribution one has to use next to leading order results, when additional gluons in the final state are present. For high  $p_T$  values processes with emission of additional gluons are suppressed by small strong coupling constant, so main contributions come from reactions with single hard gluon in the final state. For this reason we consider NLO partonic reactions  $gg \rightarrow \chi_{QJ}g$ . It should be noted, that in this approach the production of axial  $\chi_1$ -meson is possible, while at leading order it is forbidden by Landau-Yang theorem.

In our article we discuss transverse momentum distributions of  $\chi_{c,b}$  mesons. It is shown, that in the case of  $\chi_c$ -meson production our predictions agree well with the available experimental data. In case of  $\chi_b(nP)$  mesons, we give predictions of their  $p_T$ -distributions and absolute cross sections in ATLAS and LHCb experiments. One interesting property we found is that, according to our estimations, distributions of the ratios  $[d\sigma(\chi_2)/dp_T]/[d\sigma(\chi_1)/dp_T]$  for charmonium and bottomonium mesons coincide if the scaling  $p_T^{X_b} \rightarrow (M_{\chi_c}/M_{\chi_b})p_T^{X_b}$  is performed. Using existing information about radial excitation of  $\chi_b$ -mesons from different potential models we predict the ratio of  $\chi_b(2P)$  and  $\chi_b(1P)$  yields. Unfortunately, ATLAS and D0 Collaborations do not provide the information about the normalization of their results, so currently comparison with experimental data is not possible. As for newly observed  $\chi_b(3P)$  meson state, we show, that from the ratios of  $\chi_b(3P)$  and  $\chi_b(1, 2P)$  production cross sections one can determine the branching fractions of  $\chi_{b1}(3P) \rightarrow \Upsilon(1, 2S)\gamma$  decays.

## Acknowledgements

We would like to thank Dr. Vakhtang Kartvelishvili, Vladimir Obraztsov and Alexey Novoselov for useful criticism. We also want to thank colleagues from the LHCb collaboration and specially Ivan Belayev for discussions.

The work was financially supported by Russian Foundation for Basic Research (grant #10-02-00061a) and the grant of the president of Russian Federation (grant #MK-3513.2012.2).

## References

- [1] **ATLAS** Collaboration, G. Aad *et al.*, “Observation of a new  $\chi_b$  state in radiative transitions to  $\Upsilon(1S)$  and  $\Upsilon(2S)$  at ATLAS,” [arXiv:1112.5154 \[hep-ex\]](#).
- [2] **D0** Collaboration, V. M. Abazov *et al.*, “Observation of a narrow mass state decaying into Upsilon(1S) + gamma in ppbar collisions at sqrt(s) = 1.96 TeV,” [arXiv:1203.6034 \[hep-ex\]](#).
- [3] V. Kartvelishvili, A. Likhoded, and S. Slabospitsky, “D meson and Psi meson production in hadronic interactions,” *Sov.J.Nucl.Phys.* **28** (1978) 678.
- [4] S. Gershtein, A. Likhoded, and S. a. Slabospitsky, “Charmed particle inclusive spectra in photoproduction processes,” *Sov.J.Nucl.Phys.* **34** (1981) 128.
- [5] L. Gribov, E. Levin, and M. Ryskin, “Semihard Processes in QCD,” *Phys.Rept.* **100** (1983) 1–150.
- [6] S. Catani, M. Ciafaloni, and F. Hautmann, “High-energy factorization and small x heavy flavor production,” *Nucl.Phys.* **B366** (1991) 135–188.
- [7] J. C. Collins and R. Ellis, “Heavy quark production in very high-energy hadron collisions,” *Nucl.Phys.* **B360** (1991) 3–30.
- [8] B.A. Kniehl, D.V. Vasin, and V.A. Saleev, “Charmonium production at high energy in the  $k_T$  -factorization approach,” *Phys.Rev.* **D73** (2006) 074022, [arXiv:hep-ph/0602179 \[hep-ph\]](#).
- [9] **CDF** Collaboration, F. Abe *et al.*, “Production of  $J/\psi$  mesons from  $\chi_c$  meson decays in  $p\bar{p}$  collisions at  $\sqrt{s} = 1.8$  TeV,” *Phys.Rev.Lett.* **79** (1997) 578–583.
- [10] **LHCb** Collaboration, *et al.*, “Measurement of the cross-section ratio  $\sigma(\chi_{c2})/\sigma(\chi_{c1})$  for prompt  $\chi_c$  production at  $\sqrt{s} = 7$  TeV,” [arXiv:1202.1080 \[hep-ex\]](#).
- [11] R. Gastmans, W. Troost, and T. T. Wu, “Production of heavy quarkonia from gluons,” *Nucl.Phys.* **B291** (1987) 731.
- [12] P. L. Cho and A. K. Leibovich, “Color octet quarkonia production. 2.,” *Phys.Rev.* **D53** (1996) 6203–6217, [arXiv:hep-ph/9511315 \[hep-ph\]](#).
- [13] M. Klasen, B.A. Kniehl, L.N. Mihaila, and M. Steinhauser, “Charmonium production in polarized high-energy collisions,” *Phys.Rev.* **D68** (2003) 034017, [arXiv:hep-ph/0306080 \[hep-ph\]](#).

- [14] M.M. Meijer, J. Smith, and W.L. van Neerven, “Helicity amplitudes for charmonium production in hadron-hadron and photon-hadron collisions,” *Phys.Rev.* **D77** (2008) 034014, [arXiv:0710.3090 \[hep-ph\]](#).
- [15] A. Luchinsky and S. Poslavsky, “Inclusive charmonium production at PANDA experiment,” *Phys. Rev. D* **85** (Apr, 2012) 074016, [arXiv:1110.4989 \[hep-ph\]](#).
- [16] G. T. Bodwin, E. Braaten, and G. P. Lepage, “Rigorous QCD analysis of inclusive annihilation and production of heavy quarkonium,” *Phys.Rev.* **D51** (1995) 1125–1171, [arXiv:hep-ph/9407339 \[hep-ph\]](#).
- [17] . Kramer, Michael, “Quarkonium production at high-energy colliders,” *Prog.Part.Nucl.Phys.* **47** (2001) 141–201, [arXiv:hep-ph/0106120 \[hep-ph\]](#).
- [18] C. R. Munz, “Two photon decays of mesons in a relativistic quark model,” *Nucl.Phys.* **A609** (1996) 364–376, [arXiv:hep-ph/9601206 \[hep-ph\]](#).
- [19] D. Ebert, R. Faustov, and V. Galkin, “Two photon decay rates of heavy quarkonia in the relativistic quark model,” *Mod.Phys.Lett.* **A18** (2003) 601–608, [arXiv:hep-ph/0302044 \[hep-ph\]](#).
- [20] V. Anisovich, L. Dakhno, M. Matveev, V. Nikonov, and A. Sarantsev, “Quark-antiquark states and their radiative transitions in terms of the spectral integral equation. I. Bottomonia,” *Phys.Atom.Nucl.* **70** (2007) 63–92, [arXiv:hep-ph/0510410 \[hep-ph\]](#).
- [21] G.-L. Wang, “Annihilation Rate of  $2^{++}$  Charmonium and Bottomonium,” *Phys.Lett.* **B674** (2009) 172–175, [arXiv:0904.1604 \[hep-ph\]](#).
- [22] B.-Q. Li and K.-T. Chao, “Bottomonium Spectrum with Screened Potential,” *Commun.Theor.Phys.* **52** (2009) 653–661, [arXiv:0909.1369 \[hep-ph\]](#).
- [23] C.-W. Hwang and R.-S. Guo, “Two-photon and two-gluon decays of p-wave heavy quarkonium using a covariant light-front approach,” *Phys.Rev.* **D82** (2010) 034021, [arXiv:1005.2811 \[hep-ph\]](#).
- [24] **CDF** Collaboration, A. Abulencia *et al.*, “Measurement of  $\sigma(\chi(c2)B(\chi(c2) \rightarrow J/\psi\gamma))/\sigma(\chi(c1)B(\chi(c1) \rightarrow J/\psi\gamma))$  in p anti-p collisions at  $\sqrt{s} = 1.96$ -TeV,” *Phys. Rev. Lett.* **98** (2007) 232001, [arXiv:hep-ex/0703028](#).
- [25] **CMS** Collaboration, “Measurement of  $\sigma(\chi(c2))/\sigma(\chi(c1))$  at  $\sqrt{s} = 7$  tev,” CMS-PAS-BPH-11-010.
- [26] K. Nakamura *et al.* (Particle Data Group), “Review of particle physics,” *Journal of Physics G* **37** (2010) 075021. <http://pdg.lbl.gov>.
- [27] “Observation of the  $\chi_b(3P)$  state at LHCb in  $pp$  collisions at  $\sqrt{s} = 7$  TeV,” LHCb-ANA-2012-031.